View metadata, citation and similar papers at core.ac.uk

brought to you by CORE

provided by HKU Scholars Hub

The HKU Scholars Hub The University of Hong Kong 香港大學學術庫

Title	Parity of specular Andreev reflection under a mirror operation in a zigzag graphene ribbon
Author(s)	Xing, Y; Wang, J; Sun, QF
Citation	Physical Review B (Condensed Matter and Materials Physics), 2011, v. 83 n. 20, article. no. 205418 , p. 205418-1-205418-5
Issued Date	2011
URL	http://hdl.handle.net/10722/135371
Rights	Creative Commons: Attribution 3.0 Hong Kong License

Parity of specular Andreev reflection under a mirror operation in a zigzag graphene ribbon

Yanxia Xing,[1,3] Jian Wang,[1,*] and Qing-feng Sun[2,†]

[1]*Department of Physics and the Center of Theoretical and Computational Physics, The University of Hong Kong, Pokfulam Road, Hong Kong, China*

[2]*Beijing National Laboratory for Condensed Matter Physics and Institute of Physics, Chinese Academy of Sciences, 100080 Beijing, China*

[3]*Department of Physics, Beijing Institute of Technology, Beijing 100081, China*

(Received 19 January 2011; published 19 May 2011)

It is known that the parity of a reflection amplitude can either be even or odd under a mirror operation. Up to now to our knowledge, all the parities of a reflection amplitude in the one-mode energy region have been even under a mirror operation. In this paper, we give an example of odd parity for Andreev reflection (AR) in a three-terminal graphene-supercondutor hybrid system. We found that the parity is even for the Andreev retroreflection and odd for specular Andreev reflection (SAR). We attribute this remarkable phenomenon to the distinct topology of the band structure of graphene and the specular Andreev reflection involving two energy bands with different parity symmetry. As a result of the odd parity of SAR, the SAR probability of a four-terminal system with two superconducting leads (two reflection interfaces) can be 0 even when the system is asymmetric due to the quantum interference of two ARs.

DOI: 10.1103/PhysRevB.83.205418 PACS number(s): 72.80.Vp, 73.40.−c, 74.25.F−, 74.45.+c

I. INTRODUCTION

Since the experimental realization of graphene,[1] it has become an exciting arena for theoretical and technological investigations.[2] A number of new phenomena have been predicted and verified experimentally. For instance, in the presence of a magnetic field, it exhibits a distinctive half-integer quantum Hall effect.[1] Its quasiparticles obey the Dirac-like equation and have relativistic-like behaviors.[2] Due to the relativistic effect, Klein tunneling occurs where an incident electron in graphene can pass through a potential barrier with a probability of 1,[3] which induces the focusing of electron flow in a graphene p-n junction.[4,5] Besides, the well-separated valleys in a zigzag edged nanoribbon can lead to the valley valve effect.[6]

Since good contacts between superconducting leads and graphene have been realized experimentally,[7] the transport study through a graphene-based normal-metal–superconductor (GNS) heterojunction becomes feasible. In the presence of a normal metal (graphene)–superconducting interface, an incoming electron converts into a hole, and a Cooper pair is formed that enters the superconductor. Due to the relativistic nature of the electron in graphene, the electron-hole conversion can either be intraband (within the conduction or valence band) or interband (between the conduction and valence bands). When the electron-hole conversion is intraband, it corresponds to the usual Andreev reflection (AR)[8] or Andreev retroreflection (ARR) because the reflected hole is along the incident direction. This ARR occurs for both relativistic and nonrelativistic electrons. When the electron-hole conversion is interband, the reflected hole is along a specular direction and a specular Andreev reflection (SAR) takes place,[9] which can lead to novel phenomena as we will discuss below.

It is known that parity is a fundamental quantity in physics, and reflection is a general physical phenomenon in nature. In this paper, we discuss the parity of reflection amplitude for graphene in contact with superconducting leads. In general, the parity of a reflection amplitude can be either even or odd when the system is under a mirror operation. However, to our knowledge, for all previous known reflection events, the reflection amplitudes in the one-mode energy region have even parity under a mirror operation. In this paper, we found that the SAR amplitude has an odd parity under a mirror operation for zigzag graphene ribbons with even number of chains. This means that the phases of SAR amplitude for a graphene-superconductor hybrid system and its mirror system differ by π. We attribute this phenomenon to the unique band structure of the graphene. Obviously, this phase difference does not affect any observable quantities for each system. When two systems couple together, however, this π phase manifests itself through quantum interference between two SARs. So, this π phase shift has important consequences for a four-terminal device with two superconducting leads [see Fig. 2(a)]. When two superconducting leads are symmetrically attached to the device, the quantum interference of the left and right SARs leads to a destructive or constructive interference depending on whether the phase difference of superconducting leads is 0 or π. Importantly, when two superconducting leads are *asymmetrically* attached to the device, the same interference pattern occurs provided that the Dirac point E_0 is in line with the condensate of superconducting lead. The quantum interference between pairs of the AR can be tuned by shifting the Dirac point, the asymmetry of the two superconducting leads, as well as the phase between the two superconducting leads. Due to the odd parity of SAR, the interference pattern for SAR is phase contrasted to that of ARR where the parity is even.

II. THEORY AND NUMERICAL RESULTS

Before doing numerical calculations, we first prove that the phases of SAR amplitude of two systems (i) and (ii) in Fig. 1(a) differ by π, i.e., the parity of SAR is odd under a mirror operation. Note that for graphene systems, electrons in valence and conduction bands are usually referred as electrons and holes, respectively. In the presence of a superconducting lead, the reference point of electrons and holes is the Fermi level in the superconducting lead. In the following, we will refer to electrons (holes) as electrons above (below) the Fermi level

 ©2011 American Physical Society

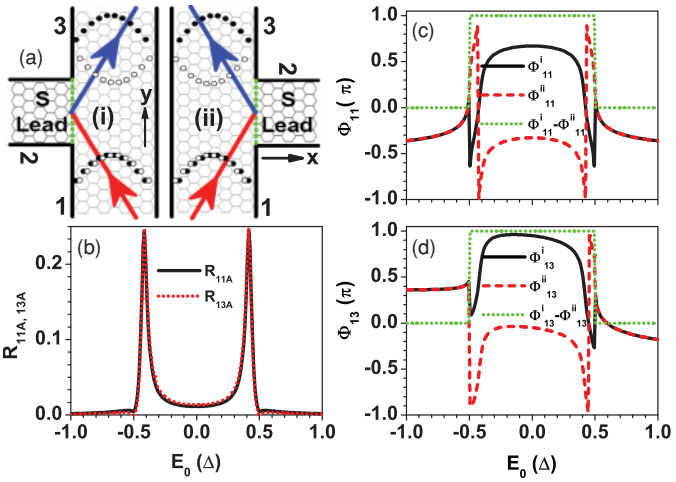

FIG. 1. (Color online) (a) Zigzag ribbons with even number of chains (gray honeycomb) attached by a superconducting lead on the left and right (orange honeycomb), respectively. For SAR, the incoming electrons (red arrow) are scattered by the GNS junction (green solid lines) as holes (blue arrows). The corresponding wave functions at sublattice "A" (solid circles) and "B" (hollow circles) for the lowest subband in the conduction band (bottom) and the highest subband in the valence band (top) are shown schematically. (b) AR probability from terminal-1 to terminal-1 R_{11A} and to terminal-3 R_{13A} vs Dirac point E_0. (c) AR phases $\Phi^{i,ii}_{11}$ and (d) $\Phi^{i,ii}_{13}$ of two systems in panel (a) and their phase differences $\Phi^{i}_{11(13)} - \Phi^{ii}_{11(13)}$ vs E_0.

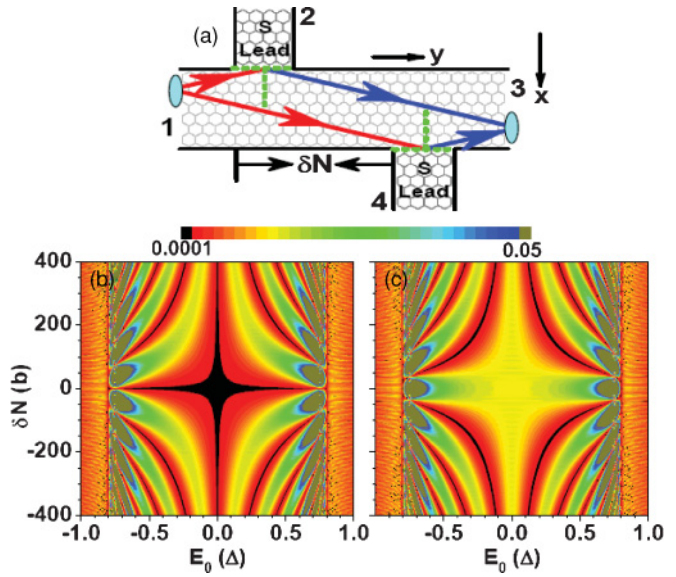

FIG. 2. (Color online) (a) Sketch of AR interferometer in which the zigzag ribbon is asymmetrically attached to two superconducting leads, lead-2 and lead-4. Electrons in terminal-1 can be Andreev reflected into terminal-3 by either the top or bottom GNS junction (horizontal green lines). (b) and (c) Contour plots of R_{13A} vs Dirac point E_0 and asymmetry δN. The phase difference between two superconducting leads $\delta\varphi$ is 0 in panel (b) and π in panel (c). The other parameters are: the Fermi energy $E_f = 0.8$, the number of chains in the zigzag ribbon $N = 40$, corresponding to width $60a$, and the width of superconducting lead $W_S = 10b$, where $b = \sqrt{3}a$.

in a superconducting lead. We denote ψ_c^+ (ψ_v^+) as the wave function of electrons in the conduction (valence) band moving in the $+y$ direction and ψ_c^- (ψ_v^-) as the wave function in the $-y$ direction in the zigzag graphene nanoribbon *lead*. It was known that under reflection $\hat{P}: x \to -x$, $\psi_c^\pm$ is symmetric while $\psi_v^\pm$ is antisymmetric if the energy of electron is in the first transmission channel[10] [see Fig. 1(a)], i.e.,

$$\begin{aligned} \hat{P}\psi_c^\pm(x,y) &= \psi_c^\pm(-x,y), \\ \hat{P}\psi_v^\pm(x,y) &= -\psi_v^\pm(-x,y), \end{aligned} \tag{1}$$

which is one of the unique features of zigzag edge nanoribbons with even number of chains. Assuming the incident electron from the terminal-1, the wave functions for SAR $\psi_{1,3}$ in zigzag nanoribbon lead-1 or lead-3 of the system (i) can be written as

$$\begin{aligned} \psi_1^{(i)} &= \psi_e^+ + r_{11}\psi_e^- + r_{11A}\psi_h^-, \\ \psi_3^{(i)} &= t_{13}\psi_e^+ + r_{13A}\psi_h^+, \end{aligned} \tag{2}$$

where r_{11} is the normal reflection amplitude, t_{13} is the transmission amplitude, and r_{11A} and r_{13A} are the Andreev reflection amplitudes with the reflected hole to the terminal-1 and terminal-3, respectively. Similarly, the wave functions for the system (ii) are given by

$$\begin{aligned} \psi_1^{(ii)} &= \psi_e^+ + \bar{r}_{11}\psi_e^- + \bar{r}_{11A}\psi_h^-, \\ \psi_3^{(ii)} &= \bar{t}_{13}\psi_e^+ + \bar{r}_{13A}\psi_h^+. \end{aligned} \tag{3}$$

Since system (i) is related to (ii) by the reflection operator $\hat{P}$, we have $\psi_\alpha^{(i)} = \hat{P}\psi_\alpha^{(ii)}$ with $\alpha = 1,3$. Note that for SAR, the electron is in the conduction band, while the hole is in the valence band, i.e., $\psi_e = \psi_c$ and $\psi_h = \psi_v$. From this relation together with Eqs. (1), (2), and (3), we obtain

$$\begin{aligned} r_{11A} &= -\bar{r}_{11A}, r_{13A} = -\bar{r}_{13A}, \\ r_{11} &= \bar{r}_{11}, t_{13} = \bar{t}_{13}. \end{aligned} \tag{4}$$

Note that the origin of this π phase shift (odd parity) is the interband conversion from the electron to the hole. Therefore, the π phase shift does not occur for ARR since it involves only intraband conversion. Now, we verify this statement numerically using a tight-binding model (see below for a detailed description of the model and numerical procedure). The numerical results of AR probability $R_{11A(13A)} = |r_{11A(13A)}|^2$ for two systems are shown in Fig. 1(b). As expected, the AR probability is exactly the same for two systems. However, the phases of AR amplitudes $r_{11A(13A)}$ that are denoted as $\Phi^{i,ii}_{11(13)}$ are different. It is shown in Figs. 1(c) and 1(c) that the ARR amplitude ($|E_0| > |E_F|$, with $|E_F| = 0.5$) is the same for the two systems in Fig. 1(a) while the SAR amplitudes ($|E_0| < |E_F|$) have a π phase shift. It confirms the odd parity for interband electron-hole conversion, which comes from the distinct topology of the band structure of graphene.

To see the consequence of the odd parity of SAR, we examine a symmetric four-terminal device with two superconducting leads depicted in Fig. 2(a) (by setting asymmetry $\delta N = 0$ and phase difference $\delta\phi = 0$). For this system, two beams from terminal-1 have a π phase shift due to odd parity of SAR and interfere destructively at terminal-3 giving rise to a vanishing SAR coefficient. However, we can arrive at

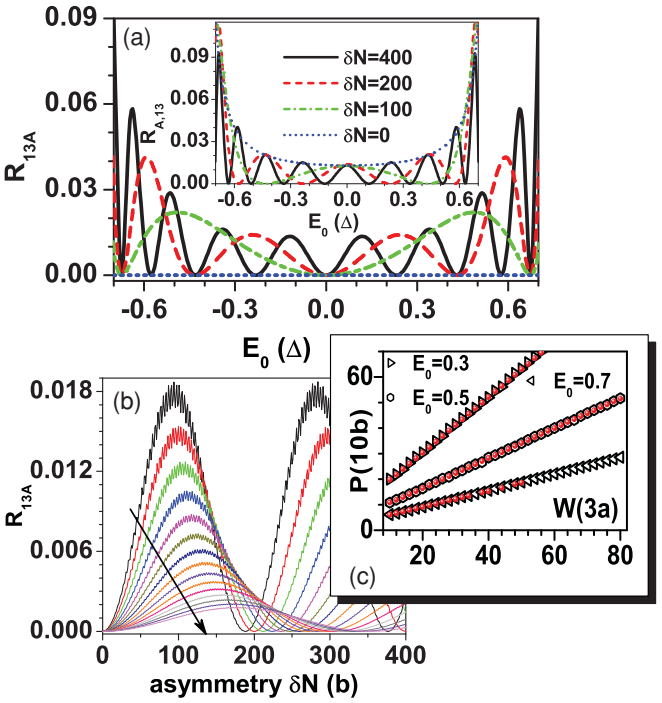

FIG. 3. (Color online) (a) With fixed Fermi level $E_F = 0.8$, total AR probability R_{13A} vs Dirac point E_0 for different asymmetries δN. In the main panel, $\delta\varphi = 0$, while $\delta\varphi = \pi$ in the inset. (b) R_{13A} vs asymmetry δN with $E_0 = 0.3t$ for different widths W from $10 \times 3a$ to $38 \times 3a$ with the interval $2 \times 3a$ along the black arrow. Inset panel: Hollow signs are the period P obtained from the main panel, and the solid red circles are the period P from the energy band with the expression $P = 2\pi/(k_x - k'_x)$. The other parameters are $\delta\varphi = 0$ and $E_F = 0.8$.

the same conclusion using a symmetry argument as follows. Since the system is symmetric with respect to $x = 0$, we must have $r_{13A} = \bar{r}_{13A}$ when the reflection operation along the x direction is applied. While from Eq. (4), $r_{13A} = -\bar{r}_{13A}$. So, the AR probability $R_{13A} = |r_{13A}|^2$ for SAR can also be 0 from a symmetry point of view.[11] Therefore, we conclude that the symmetric device can not be used to test the odd parity of SAR. In the following, we demonstrate that due to the π phase shift, the destructive interference still occurs in four-probe devices with two superconducting leads attached asymmetrically and, hence, can be used to test the odd parity of SAR.

For this purpose, we consider an asymmetric four-terminal device consisting of a zigzag graphene ribbon with two superconducting leads as shown in Fig. 2(a). The Hamiltonian of the graphene is[12] $H_0 = \sum_{\mathbf{i}} \epsilon_{\mathbf{i}} a_{\mathbf{i}}^\dagger a_{\mathbf{i}} - \sum_{\langle \mathbf{ij} \rangle} t a_{\mathbf{i}}^\dagger a_{\mathbf{j}}$. Here, $a_{\mathbf{i}}$ and $a_{\mathbf{i}}^\dagger$ are the annihilation and creation operators, respectively, at site $\mathbf{i}$, $\epsilon_{\mathbf{i}}$ is the on-site energy which can be controlled experimentally by the gate voltage,[1] and the hopping constant $t = 2.75$ eV represents the nearest carbon bond energy. The pair potential (energy gap) of superconducting terminal-β with $\beta = 2,4$ is $\tilde{\Delta}_\beta = \Delta_\beta e^{i\varphi_\beta}$ with $\Delta_2 = \Delta_4 = \Delta \simeq 1$ meV. In numerical calculations,[11] we fix Fermi energy E_F and tune the Dirac point E_0. We have used Δ as the energy unit.

Now, we study the interference between two ARs from the GNS junctions as shown in Fig. 2(a) in which two superconducting leads, lead-2 and lead-4, are asymmetrically

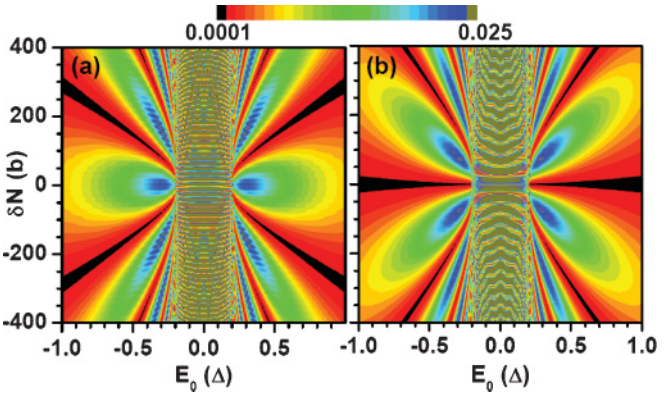

FIG. 4. (Color online) Interference pattern of AR from terminal-1 to terminal-1. The phase difference of the two superconducting leads is (a) 0 and (b) π. The other parameters are same as in Fig. 2, except for $E_F = 0.2$.

attached to the zigzag nanoribbon. The horizontal distance δN between the two GNS junctions measures the asymmetry of the two GNS junctions. The scattering process can be qualitatively understood as follows. For simplicity, we assume $\phi_2 = \phi_4$ for the moment. As shown schematically in Fig. 2(a), for SAR, the particlelike electrons in terminal-1 split into two beams and are scattered separately by the two GNS junctions (green horizontal lines) as holes that finally recombine at terminal-3. We examine the total phase accumulated for each beam that involves the following three processes. Before reaching the first GNS junction (intersection of left horizontal and vertical green lines), the two beams of electrons propagate with the same momentum k_x. After reaching the second GNS junction (intersection of right horizontal and vertical green lines), two beams of holes also propagate with the same momentum k'_x. Obviously, phases accumulated in the above two processes for both beams are the same. Between them, the two beams propagate with different momenta k_x and k'_x. Hence, the phase difference between the two beams is $\phi = (k_x - k'_x)\delta x$ with $\delta x = b\delta N$, where $b = \sqrt{3}a$ and a is the lattice constant. This phase difference can be tuned by varying the Dirac point E_0 or the asymmetry δN giving rise to a complicated interference pattern (see Fig. 2). In particular, this phase difference can be 0 if $(k_x - k'_x) = 0$ (i.e., $E_0 = 0$) or $\delta N = 0$. In general, the total phase difference is $\phi = (k_x - k'_x)\delta x + \phi_2 - \phi_4$.

The interference patterns of AR probability R_{13A} for the system depicted in Fig. 2(a) with pair potential phase differences of two superconductors $\delta\varphi = 0$ and π ($\delta\varphi \equiv \varphi_2 - \varphi_4$) are then plotted in Figs. 2(b) and 2(c), respectively.

For Fig. 2(b), the following observations are in order:

(1) For the geometrically symmetric system ($\delta N = 0$), the interference is always destructive with zero R_{13A} as long as $|E_0| < |E_F|$.[11] Clearly, this is due to the π phase shift depicted in Fig. 1(d) and is consistent with the band selection rule.[10]

(2) When Dirac point E_0 is in line with the condensate energy of the superconductor, i.e., when $E_0 = 0$, R_{13A} is again 0 no matter what value δN assumes. This means that there is a completely destructive interference between the two beams scattered by the two GNS junctions attached asymmetrically to the graphene nanoribbon. This behavior can be understood as follows. When $E_0 = 0$, the incoming electron and reflected

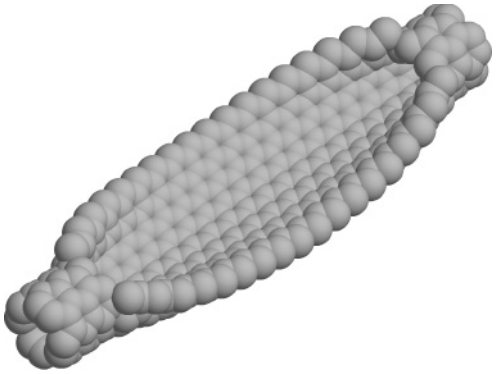

FIG. 5. Schematic plot of partially unzipped CNT.

hole have the same propagating momentum k_x, and thus paths 1 and 2 in Fig. 2(a) experience the same quantum phase $k_x\delta x$, except at the superconducting leads. Hence, the total phase difference is only due to the π phase shift between two SARs.

(3) R_{13A} is an even function of Dirac point E_0 because of the electron-hole symmetry in graphene. Due to the geometric symmetry, R_{13A} is also an even function of asymmetry δN.

(4) For nonzero E_F, the closer the Dirac point E_0 to E_F, the more rapidly R_{13A} oscillates as we vary δN. This is because the difference of propagating momentum $k_x - k'_x$ increases monotonically as E_0 approaches E_F.

(5) When E_0 is in the vicinity of E_F, R_{13A} can reach 0.9, which is much larger than that when $|E_0| > |E_F|$. This is because when E_F is very close to E_0, the edge states of the zigzag ribbon begin to contribute; then, it is easier for electrons to be scattered by the two GNS junctions located also at the edges of the zigzag ribbon. Considering the pseudospin conservation, large R_{13A} is always found in the region of $|E_0| < |E_F|$, i.e., the SAR region.

(6) There is an overall fine oscillation with a period of $\delta N = 3b$. Similar behavior was also found in zigzag ribbons with a p-n junction where the conductance is determined by the relative displacement δ along the p-n junction.[13]

In Fig. 2(c), with the superconducting phase difference $\delta\varphi = \pi$, we see that the interference pattern reverses at $\delta\varphi = 0$ [Fig. 2(b)] where the constructive interference becomes destructive and vice versa.

To further analyze the interference pattern, we plot in Fig. 3(a) the total R_{13A} vs Dirac point E_0 for different asymmetries δN with the phase difference between the two superconducting leads, $\delta\varphi = 0$ [main panel of Fig. 3(a)] or $\delta\varphi = \pi$ [inset of Fig. 3(a)]. Clearly, the interference (oscillatory) pattern occurs only for asymmetric systems ($\delta N \neq 0$) with oscillation frequency proportional to δN. When pair potential phase difference $\delta\varphi = \pi$ is introduced, the interference pattern reverses, and R_{13A} with $\delta N = 0$ becomes the envelope function of R_{13A} for all nonzero δN. In Fig. 3(b), we plot R_{13A} vs δN for different widths W of the nanoribbon. It is shown clearly that R_{13A} is a periodic function of δN with larger periodicity for larger W. In the inset of Fig. 3(b), we plot this period versus the width for different E_0. The period P is obtained in two ways:

(1) from the expression $P = 2\pi/(k_x - k'_x)$ where the momenta k_x and k'_x can be obtained from the band structure for a given E_0 (◯ symbols);

(2) directly from main panel of Fig. 3(b) (red solid circles). The inset clearly shows that the two periods are exactly the same, giving strong evidence that the interference patterns of AR probability are indeed from the two reflected hole beams.

Finally, the interference pattern of AR probability R_{11A} is also studied (Fig. 4). We found that only ARR probability R_{11A} ($|E_0| > E_F = 0.2\Delta$) exhibits an interference pattern. We note that since there is no π phase shift involved in ARR, when $\delta N = 0$, reflected electrons through two the GNS junctions interfere constructively when $\delta\varphi = 0$, and destructively when $\delta\varphi = \pi$, which is in contrast to SAR in Fig. 2. In fact, interference patterns of SAR and ARR are always phase contrast, not only for $\delta N = 0$, but also for all other δN.

To test the odd parity of SAR experimentally, physicists require the fabrication of high quality zigzag graphene nanoribbons. This was achieved last year by several laboratories using different methods, including the method to unzip the carbon nanotube (CNT),[14] the method of anisotropic etching by thermally activated nickel nanoparticles,[15] and the use of chemical method[16] and reconstruction of the edge[17] to make zigzag graphene nanoribbons. In view of the above experimental breakthrough, we expect that the setup to test our predicted phenomenon can be realized experimentally.

To reduce the experimental challenge, we have considered an unzipped CNT device, i.e., an (n,n) CNT-zigzag graphene-(n,n) CNT, obtained by unzipping a few unit cells in the central part of an armchair CNT, which has been achieved experimentally (see Fig. 5).[14] For this system, the wave function in the armchair CNT has the same symmetry as that of the zigzag graphene ribbon. Following the same procedure leading to Eq. (4), we have shown that the unzipped CNT in contact with a superconducting lead has odd parity under a mirror operation. Similar conclusions drawn from a GNS can be obtained an for unzipped CNT with two superconducting leads.

III. CONCLUSION

In conclusion, up to now to our knowledge, the parity of a reflection amplitude was found to be even under a mirror operation. Here, we have provided an example of odd parity for a reflection amplitude, the SAR amplitude in the zigzag graphene-superconductor hybrid system. This odd parity is due to the combination of the unique band structure of the graphene and the electron-hole conversion involving two energy bands with different parity symmetries. The signature of odd parity of SAR can be found from the quantum constructive interference in a four-terminal system with two superconducting leads attached asymmetrically. Furthermore, the interference pattern due to the odd parity of a SAR is phase contrasted to that of an ARR where the parity is even.

ACKNOWLEDGMENTS

We gratefully acknowledge the financial support from RGC (HKU 705409P) and University Grant Council (Contract No. AoE/P-04/08) of the Government of HKSAR, from NSF-China under Grant Nos. 10 974 236 and 10 821 403, and excellent young scholars research fund of Beijing Institute of Technology.

*jianwang@hkusua.hku.hk
†sunqf@aphy.iphy.ac.cn

[1]K. S. Novoselov, A. K. Geim, S. V. Morozov, D. Jiang, Y. Zhang, S. V. Dubonos, I. V. Grigorieva, and A. A. Firsov, Science **306**, 666 (2004); K. S. Novoselov, A. K. Geim, S. V. Morozov, D. Jiang, M. I. Katsnelson, I. V. Grigorieva, S. V. Dubonos, and A. A. Firsov, Nature (London) **438**, 197 (2005); Y. Zhang, Y.-W. Tan, H. L. Stormer, and P. Kim, *ibid.* **438**, 201 (2005).

[2]C. W. J. Beenakker, Rev. Mod. Phys. **80**, 1337 (2008); A. H. Castro Neto, F. Guinea, N. M. R. Peres, K. S. Novselov, and A. K. Geim, *ibid.* **81**, 109 (2009).

[3]M. I. Katsnelson, K. S. Novoselov, and A. K. Geim, Nature Phys. **2**, 620 (2006); A.-F. Young *et al.*, *ibid.* **5**, 222 (2009); A. V. Shytov, M. S. Rudner, and L. S. Levitov, Phys. Rev. Lett. **101**, 156804 (2008).

[4]V. V. Cheianov *et al.*, Science **315**, 1252 (2007).

[5]Y. Xing, J. Wang, and Q.-F. Sun, Phys. Rev. B **81**, 165425 (2010).

[6]A. Rycerz, J. Tworzydło, and C. W. J. Beenakker, Nature Phys. **3**, 172 (2007).

[7]H. B. Heersche, P. Jarillo-Herrero, J. B. Oostinga, L. M. K. Vandersypen, and A. F. Morpurgo, Nature (London) **446**, 56 (2007); F. Miao, S. Wijeratne, Y. Zhang, U. C. Coskun, W. Bao, and C. N. Lau, Science **317**, 1530 (2007).

[8]A. F. Andreev, Sov. Phys. JETP **19**, 1228 (1964).

[9]C. W. J. Beenakker, Phys. Rev. Lett. **97**, 067007 (2006).

[10]J. Nakabayashi, D. Yamamoto, and S. Kurihara, Phys. Rev. Lett. **102**, 066803 (2009).

[11]S. Cheng,Y. Xing, J. Wang, and Q. F. Sun, Phys. Rev. Lett. **103**, 167003 (2009); Q.-F. Sun and X. C. Xie, J. Phys. Condens. Matter **21**, 344204 (2009).

[12]D. N. Sheng, L. Sheng, and Z. Y. Weng, Phys. Rev. B **73**, 233406 (2006); Z. Qiao and J. Wang, Nanotechnology **18**, 435402 (2007); W. Long, Q.-F. Sun, and J. Wang, Phys. Rev. Lett. **101**, 166806 (2008); J. Li and S.-Q. Shen, Phys. Rev. B **78**, 205308 (2008).

[13]A. R. Akhmerov, J. H. Bardarson, A. Rycerz, and C. W. J. Beenakker, Phys. Rev. B **77**, 205416 (2008).

[14]L. Jiao, L. Zhang, X. Wang, G. Diankov, and H. Dai, Nature (London) **458**, 877 (2009); D. V. Kosynkin, A. L. Higginbotham, A. Sinitskii, J. R. Lomeda, A. Dimiev, B. K. Price, and J. M. Tour, *ibid.* **458**, 872 (2009).

[15]L. C. Campos, V. R. Manfrinato, J. D. Sanchez-Yamagishi, J. Kong, and P. Jarillo-Herrero, Nano Lett. **9**, 2600 (2009).

[16]X. Li, X. Wang, L. Zhang, S. Lee, and H. J. Dai, Science **319**, 1229 (2008).

[17]X. Jia, M. Hofmann, V. Meunier, B. G. Sumpter, J. Campos-Delgado, J. M. Romo-Herrera, H. Son, Y.-P. Hsieh, A. Reina, J. Kong, M. Terrones, and M. S. Dresselhaus, Science **323**, 1701 (2009); Ç. Ö. Girit, J. C. Meyer, R. Erni, M. D. Rossell, C. Kisielowski, L. Yang, C.-H. Park, M. F. Crommie, M. L. Cohen, S. G. Louie, and A. Zettl, *ibid.* **323**, 1705 (2009).